NiO–polyoxometalate nanocomposites as efficient catalysts for the oxidative dehydrogenation of propane and isobutane†

Qinghong Zhang, Chuanjing Cao, Ting Xu, Miao Sun, Jizhe Zhang, Ye Wang* and Huilin Wan*

Received (in Cambridge, UK) 5th January 2009, Accepted 20th February 2009
First published as an Advance Article on the web 12th March 2009
DOI: 10.1039/b823369a

Novel nanocomposites of NiO and polyoxometalate ($Cs_{2.5}H_{0.5}PMo_{12}O_{40}$) with particle sizes in the range of 5–10 nm showed exceptional oxygen and ammonia adsorption capabilities, and the nanocomposites catalyzed the oxidative dehydrogenation of propane and isobutane efficiently under mild conditions.

Selective oxidation of light alkanes into olefins and organic oxygenates is an attractive route for the utilization of abundant light alkane resources. Although intensive efforts have been made in this field, selective oxidation of C_1–C_4 alkanes still remains an unsolved challenge, except for the conversion of *n*-butane to maleic anhydride.[1] The main reason is that the alkane activation generally requires severe conditions, under which the consecutive oxidation of reactive target products to CO and CO_2 can easily occur, leading to low selectivities to target products at reasonably high conversions.[2] Therefore, the development of efficient catalysts which are capable of working under mild conditions would be a promising route.

NiO is a typical p-type semiconductor, and various types of oxygen species can be adsorbed on its surface under mild conditions.[3] Some studies have shown that NiO can work for the oxidative dehydrogenation (ODH) of light alkanes at mild temperatures (<500 °C).[4] However, because NiO can be easily reduced to Ni^0, single NiO is hard to employ as a stable catalyst with high catalytic performances. Some composite oxides such as Ni–Ce–O, Ni–Nb–O and Ni–Ti–O with relatively higher stability toward reduction have been investigated for the ODH of ethane or propane, but olefin yields are still not satisfactory.[5] For the ODH of propane, the highest propene yield over these composites was $\sim$12%.[5c,d] On the other hand, polyoxometalates, which have received considerable attention in materials science, catalysis and biological fields,[6] are well known to have the ability to activate molecular oxygen at moderate temperatures, and some substituted polyoxometalates have been exploited for the selective oxidation of light alkanes.[7] It would be of interest to combine the advantages of both NiO and polyoxometalates. Recently, we have succeeded in synthesizing nanocomposites of NiO and a polyoxometalate ($Cs_{2.5}H_{0.5}PMo_{12}O_{40}$, denoted as POM) with excellent catalytic performances in the ODH of propane and isobutane. Herein, we report the structure, adsorption properties and catalytic behaviour of the NiO–POM nanocomposites.

NiO–POM composites with different compositions were synthesized by a citric acid complexation method (see ESI† for details). We fixed the composition of POM at $Cs_{2.5}H_{0.5}PMo_{12}O_{40}$ here because the composites containing POM with this composition showed outstanding catalytic performances and good stability. XRD patterns of the NiO–POM composites are shown in Fig. 1. For the composites with NiO content of 85–75 wt% and POM content of 15–25 wt% (denoted as 85–75% NiO–POM), only diffraction peaks of NiO could be observed. Moreover, these diffraction peaks became much broader compared with those of single NiO, indicating that the crystalline size of NiO in these composites became smaller. With further decrease of NiO content to $\leq$70 wt% in the composites, XRD peaks of NiO became weaker and those of POM appeared.

SEM and TEM observations suggest that the size and morphology of the NiO–POM composites are different from those of single compounds. Fig. 2 and 3 show that the 80% and 70% NiO–POM samples are composed of uniform nanoparticles with sizes of 5–10 nm, which are much smaller than those of single NiO ($\sim$26 nm) or $Cs_{2.5}H_{0.5}PMo_{12}O_{40}$

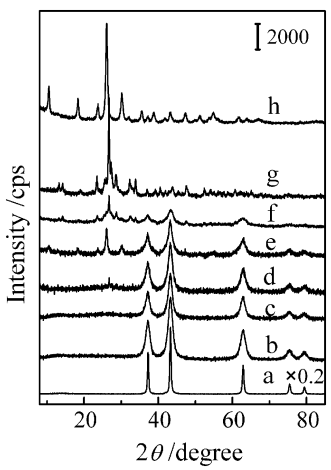

Fig. 1 XRD patterns. (a) NiO, (b) 85% NiO–POM, (c) 80% NiO–POM, (d) 75% NiO–POM, (e) 70% NiO–POM, (f) 50% NiO–POM, (g) 30% NiO–POM, (h) POM ($Cs_{2.5}H_{0.5}PMo_{12}O_{40}$).

State Key Laboratory of Physical Chemistry of Solid Surfaces, National Engineering Laboratory for Green Chemical Productions of Alcohols, Ethers and Esters, College of Chemistry and Chemical Engineering, Xiamen University, Xiamen, 361005, China. E-mail: wangye@xmu.edu.cn, hlwan@xmu.edu.cn; Fax: +86-59-2183047; Tel: +86-592-2186156

† Electronic supplementary information (ESI) available: Experimental details, EDS results, BET surface areas, adsorption amounts of O_2 and NH_3, FT-IR spectra of adsorbed NH_3, plots of selectivity *versus* conversion, catalytic stability and FT-IR spectra before and after reactions. See DOI: 10.1039/b823369a

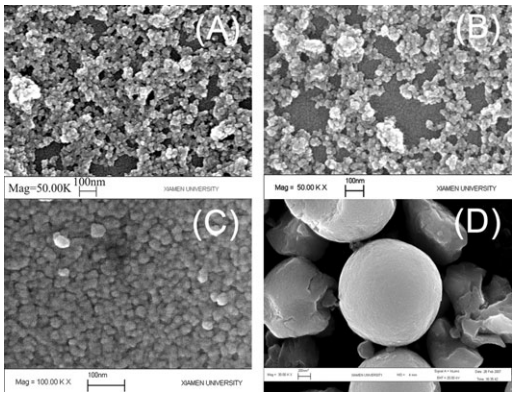

Fig. 2 SEM images. (A) 80% NiO–POM, (B) 70% NiO–POM, (C) NiO, (D) POM ($Cs_{2.5}H_{0.5}PMo_{12}O_{40}$). The scale bar in (A)–(C) denotes 100 nm, while that in (D) denotes 200 nm.

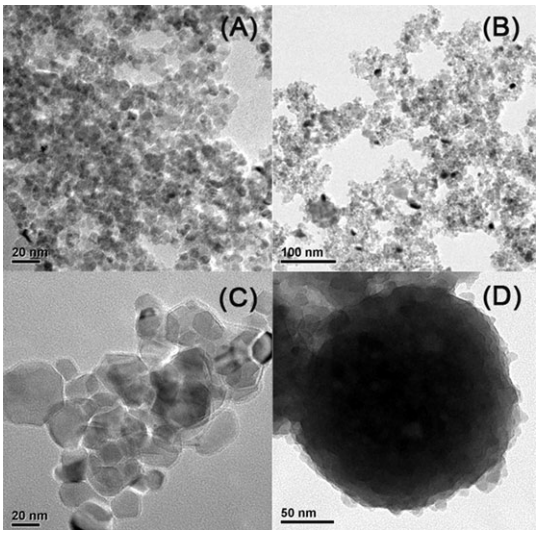

Fig. 3 TEM images. (A) 80% NiO–POM, (B) 70% NiO–POM, (C) NiO, (D) POM ($Cs_{2.5}H_{0.5}PMo_{12}O_{40}$).

(1–2 μm). EDS analyses revealed that all the elements including Ni, Cs, P, Mo and O distributed homogeneously over the NiO–POM composite (see Fig. S1, ESI†). The surface areas of the 85–70% NiO–POM composites were larger than those of single NiO and POM (see Table S1, ESI†).

We found that the NiO–POM nanocomposites showed interesting oxygen adsorption behaviour. For single NiO, we observed three O_2 desorption peaks at 220, 325 and 490 °C in the O_2–TPD profile (Fig. 4A). These peaks were reported to arise from the oxygen species chemisorbed on NiO surface and were assigned to O_2^- (the first peak) and O^- species (the second and the third peaks).[3] On the other hand, there was almost no desorption of O_2 from the POM. For the 85% and 80% NiO–POM nanocomposites, the O_2 desorption pattern was the same as that of NiO, but the desorption temperatures increased by ~200 °C. This indicates that the oxygen species become more stable than those on single NiO. The amount of O_2 adsorbed per gram of sample for these two nanocomposites was larger than that for single NiO although the adsorption amount per surface area became lower for the nanocomposites (see Table S2, ESI†). To our knowledge, the effort to improve

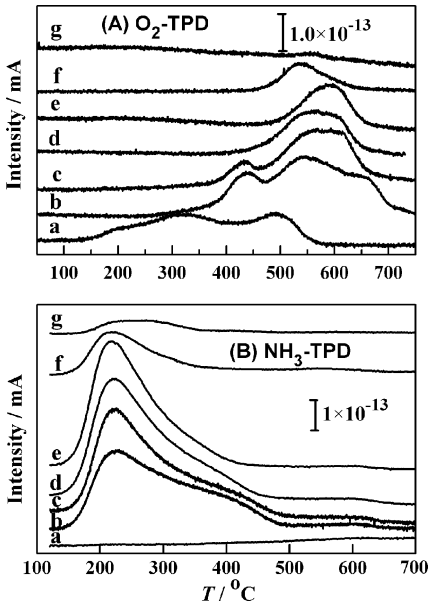

Fig. 4 O_2–TPD and NH_3–TPD profiles. (a) NiO, (b) 85% NiO–POM, (c) 80% NiO–POM, (d) 75% NiO–POM, (e) 70% NiO–POM, (f) 50% NiO–POM, (g) POM ($Cs_{2.5}H_{0.5}PMo_{12}O_{40}$).

the stability of adsorbed oxygen on NiO by combining other oxides always leads to marked decrease in the amount of oxygen adsorption even based on the same amount (gram) of sample.[5]

We found an unexpected NH_3 adsorption ability of the NiO–POM nanocomposites. NH_3–TPD results in Fig. 4B show that there is no or only a small amount of NH_3 adsorption over single NiO or POM. However, a large amount of NH_3 desorption was observed at 150–500 °C over the NiO–POM nanocomposites with NiO contents of 85–70%. As compared to single POM, the nanocomposites exhibited significantly higher amount of NH_3 adsorption per surface area (see Table S2, ESI†). FT-IR studies of adsorbed NH_3 suggest that the acidic sites over the nanocomposites are mainly the Lewis type in nature, whereas the POM possesses mainly the Brønsted acid sites (see Fig. S2, ESI†).

We have investigated the chemical states of Ni and Mo in the NiO–POM nanocomposites by XPS studies. In the 80% NiO–POM, the binding energy (E_B) of Ni_{2p} was at 854.2 eV, which was higher than that in single NiO (E_B = 853.8 eV). The E_B of Mo $3d_{5/2}$ in the composite was at 232.4 eV, lower than that in $Cs_{2.5}H_{0.5}PMo_{12}O_{40}$ (E_B = 232.9 eV). This suggests the partial oxidation of Ni^{2+} to Ni^{3+} and the partial reduction of Mo^{6+} to Mo^{5+} in the nanocomposite.[8] Thus, an electron transfer from Ni^{2+} to Mo^{6+} sites may occur in the composite. We speculate that there may also be a migration of oxygen anion from Mo to Ni sites, leaving oxygen vacancies around the coordinatively unsaturated Mo^{5+} sites. This may create a number of oxygen species on NiO phase near Ni^{3+} sites in the nanocomposite. Because of the strong interaction with the POM component, the oxygen species on NiO may become more stable than those on single NiO. The coordinatively unsaturated Mo^{5+} sites probably function as the Lewis acid sites responsible for the unique NH_3 adsorption over the NiO–POM composite. These Mo^{5+} sites may also work for the adsorption and activation of molecular oxygen.

Table 1 shows the catalytic performances of the NiO–POM nanocomposites for the ODH of propane at 450 °C. Single NiO only catalyzed the formation of CO and CO_2 under the conditions in Table 1, whereas single POM showed a very low propane conversion. The NiO–POM nanocomposites could catalyze the selective formation of propene at good propane conversions. Moreover, the nanocomposite prepared by the citric acid complexation method exhibited much higher selectivity than the corresponding physical mixture of NiO and POM. We further compared propene selectivities over the 80% NiO–POM and NiO at different propane conversions, and the result confirmed that the 80% NiO–POM was a significantly more selective catalyst for the ODH of propane (see Fig. S3, ESI†). The 80% NiO–POM catalyst was found to be stable during the reaction, and the propene yield did not undergo significant changes with time on stream (see Fig. S4, ESI†). To our knowledge, the propene yield (20%) obtained over the present nanocomposite is the highest one reported to date under such a mild temperature. Furthermore, our FT-IR studies for the NiO–POM composites before and after the catalytic reaction under conditions of Table 1 indicated that there was no significant change in the structure of the nanocomposites (see Fig. S5, ESI†).

The NiO–POM nanocomposites also showed superior catalytic performances for the ODH of isobutane. Over the 70% NiO–POM nanocomposite, the selectivities to isobutene were 79% and 71% at isobutane conversions of 15% and 21% at 450 and 500 °C, respectively (Table 2). The total selectivity to isobutene and methacrolein reached 90% and 82% at the same time. These performances are significantly better than those reported for other catalysts.[9] The 70% NiO–POM was also stable during the ODH of isobutane (see Fig. S6, ESI†). We suggest that the superior performances of the NiO–POM nanocomposites in the ODH reactions are related to the enhanced stability of the oxygen species. Moreover, the disappearance of O_2^- species over the nanocomposites with NiO content $\leq$75 wt% (Fig. 4A) may also contribute to their higher selectivity.

In conclusion, we have succeeded in synthesizing a NiO–POM nanocomposite with particle sizes in the range of 5–10 nm. The nanocomposite exhibits unique capabilities for the adsorption of oxygen and ammonia and superior catalytic behaviours in the ODH of propane and isobutane. A stable propene yield of 20% can be obtained in the ODH of propane at 450 °C. For the ODH of isobutane, the selectivity to isobutene and methacrolein reaches 90% at an isobutane conversion of 15%.

Table 1 Catalytic performances of the NiO–POM nanocomposites for the oxidative dehydrogenation of propane[a]

Catalyst	Conv./%	Selectivity[b]/%			C_3H_6 yield/%
		C_3H_6	CO	CO_2	
NiO	100	0	13	59	0
85% NiO–POM	72	20	0	80	8.2
80% NiO–POM	44	45	4.6	50	20
75% NiO–POM	23	65	6.4	27	15
70% NiO–POM	11	75	5.9	16	8.2
50% NiO–POM	3.0	81	2.2	17	2.4
POM	1.5	95	1.9	3.0	1.4
80% NiO–POM[c]	55	14	0	86	7.9

[a] Reaction conditions: T = 450 °C; W = 0.5 g; $P(C_3H_8)$ = 4.1 kPa; $P(O_2)$ = 16.2 kPa; $P(N_2)$ = 81.1 kPa; F(total) = 50 mL min^{-1}. [b] Other products mainly include CH_4, C_2H_6 and C_2H_4. [c] Prepared by physical mixing.

Table 2 Catalytic performances of the NiO–POM nanocomposites for the oxidative dehydrogenation of isobutane[a]

Catalyst	Temp./°C	Conv./%	Selectivity[b]/%		
			i-C_4H_8	MA[c]	CO_2
NiO	400	43	11	0	67
	450	50	0	0	69
80%NiO–POM	400	16	63	0	38
	450	48	20	0	80
70%NiO–POM	450	15	79	11	10
	500	21	71	11	18
50% NiO–POM	450	4.7	93	0	7
	500	8.4	87	0	13
POM	400	$<$1.0	—	—	—

[a] Reaction conditions: W = 0.5 g; $P(i\text{-}C_4H_{10})$ = 5.6 kPa; $P(O_2)$ = 11.2 kPa; $P(N_2)$ = 84.2 kPa; F(total) = 90 mL min^{-1}. [b] Other products are mainly CH_4. [c] MA denotes methacrolein.

This work was supported by the NSFC (No. 20625310, 20773099 and 20873110), the National Basic Research Program of China (No. 2005CB221408), and the Program for New Century Excellent Talents in Fujian Province (Q.Z.).

Notes and references

1 F. Cavani, N. Ballarini and A. Cericola, *Catal. Today*, 2007, **127**, 113.
2 F. E. Cassidy and B. K. Hodnett, *CATTECH*, 1998, **2**, 173.
3 (*a*) M. Iwamoto, Y. Yoda, M. Egashira and T. Seiyama, *J. Phys. Chem.*, 1976, **80**, 1989; (*b*) A. Bielanski and M. Najbar, *J. Catal.*, 1972, **25**, 398.
4 (*a*) M. Zhang, J. Liu, C. Liu, R. Lan, L. Ji and X. Chen, *J. Chem. Soc., Chem. Commun.*, 1993, 1480; (*b*) Y. Schuurman, V. Ducarme, T. Chen, W. Li, C. Mirodatos and G. A. Martin, *Appl. Catal., A*, 1997, **163**, 227; (*c*) X. Zhang, J. Liu, Y. Jing and Y. Xie, *Appl. Catal., A*, 2003, **240**, 143.
5 (*a*) P. Boizumault-Moriceau, A. Pennequin, B. Grzybowska and Y. Barbaux, *Appl. Catal., A*, 2003, **245**, 55; (*b*) E. Heracleous and A. A. Lemonidou, *J. Catal.*, 2006, **237**, 162; (*c*) Y. Wu, Y. He, T. Chen, W. Weng and H. Wan, *Appl. Surf. Sci.*, 2006, **252**, 5220; (*d*) Y. He, Y. Wu, T. Chen, W. Weng and H. Wan, *Catal. Commun.*, 2006, **7**, 268.
6 (*a*) A. Proust, R. Thouvenot and P. Gouzerh, *Chem. Commun.*, 2008, 1837; (*b*) E. Cartuyvels, G. Absillis and T. Parac-Vogt, *Chem. Commun.*, 2008, 85.
7 (*a*) T. Okuhara, N. Mizuno and M. Misono, *Adv. Catal.*, 1996, **41**, 113; (*b*) N. Mizuno and D. Suh, *Appl. Catal., A*, 1996, **146**, L249; (*c*) N. Dinmitratos and J. C. Vèdrine, *Appl. Catal., A*, 2003, **256**, 251; (*d*) F. Cavani, R. Mezzogori, A. Pigano and F. Trifiró, *Top. Catal.*, 2003, **23**, 119; (*e*) Dinmitratos and J. C. Vèdrine, *Catal. Commun.*, 2006, **7**, 811; (*f*) M. Sun, J. Zhang, C. Cao, Q. Zhang, Y. Wang and H. Wan, *Appl. Catal., A*, 2008, **349**, 212.
8 (*a*) S. Uhlenbrock. C. Scharfschwerdt, M. Neumann, G. Illing and H. Freund, *J. Phys.: Condens. Matter*, 1992, **4**, 7973; (*b*) J. Swiatowska-Mrowiecka, S. Dieshach, V. Maurice, S. Zanna, L. Klein, E. Briand, I. Vickridge and P. Marcus, *J. Phys. Chem. C*, 2008, **112**, 11050.
9 (*a*) F. Cavani, C. Comuzzi, G. Dolcetti, E. Etienne, R. Finke, G. Selleri, F. Trifirò and A. Trovarelli, *J. Catal.*, 1996, **160**, 317; (*b*) Y. Takita, X. Qing, A. Takami, H. Nishhiguchi and K. Nagaoka, *Appl. Catal., A*, 2005, **296**, 63; (*c*) L. Huerta, P. Amorós, D. Beltrán-Porter and V. Corberán, *Catal. Today*, 2006, **117**, 180.

